To Deuterate Your Proteins or Not to Deuterate? That is the Question.

by Bibhuti Das, Paul Ellis, and F. David Doty

High-resolution inverse ^{1}H detection in solid-state (ss) NMR spectroscopy is rapidly evolving with the development of fast magic angle spinning (MAS) probes and protein biochemistry. Fast MAS ($\nu_R > 40$ kHz) partially averages the homonuclear dipolar network of ^{1}Hs by spinning the sample rapidly at magic angle (54.7356˚). The latter approach is more applicable to ss-NMR of proteins where the dense ^{1}H-^{1}H dipolar network is diluted with inclusion of ^{2}H during biosynthesis of proteins. With the advent of fast spinning three channel probes (fixed tune H, C, and N and $\nu_R > 100$ kHz with 0.7 mm rotors), a strategy is evolving. One approach suggests the sample need not be deuterated at all, simply spin fast enough to average the homonuclear dipolar networks. Another approach involves a larger sample (1.3 mm as opposed to 0.7 mm rotors) and subsequently spin the sample with rates between 40 and 60 kHz and employ novel biochemical means of deuteration to improve the overall resolution. Experimental demonstration indicates that perdeuteration or ^{2}H labeling up to 70% (30% overall protonation) has improved resolution below 25 Hz for methyl and amide protons even under moderate spinning speed (25 kHz). An alternative to these approaches is to employ even larger 3 mm sample (1.9 mm in the future) and spin at more modest rates (25 kHz- 28 kHz in the case of 3 mm rotors). Further, the 3 mm probe employs features that facilitate higher resolution. In this case, the novel design utilizes 4 channels (the usual H, C, and N) while the 4th channel in this case providing ^{2}H decoupling and hence gaining substantial resolution benefits by removing ^{1}H-^{2}H line broadening due to heteronuclear J-coupling. In this white paper we will discuss the advantages and disadvantages of each strategy. A tacit assumption of all three strategies and their respective probes is that they can be extended to the highest magnetic fields.

Why fast MAS?

Spinning a sample at magic angle will time average the anisotropic interactions such as chemical shift anisotropy and dipole-dipole couplings. We mentioned briefly above one strategy to obtain a high resolution ^{1}H spectrum was simply to spin fast without added ^{2}H. Why do we have to spin fast? The origins of the answer to that question lies in a series of classic "hole burning" experiments by Portis.[1] The original experiments by Portis, were carried out EPR resonances. We simply have transferred his reasoning to ^{1}H and ^{13}C resonances. It was noted that if you applied CW rf irradiation to a ^{13}C lineshape, the resulting lineshape developed a "notch" at the point of irradiation. The ^{13}C lineshape was denoted as inhomogeneous.[1] In contrast if the same experiment is applied to a ^{1}H lineshape, the resonance saturates and disappears. This lineshape is described as homogeneous. Why the difference? In the case of ^{13}C, the natural abundance is so low (1.1%) that it can be considered a rare spin. The carbons feel the influence of the heteronuclear dipolar interaction arising from the ^{1}Hs, however, as a routine part of the experiment the ^{1}Hs are decoupled with a strong resonant rf irradiation. Hence, the carbons are an isolated spin system. If you consider the lineshape as composed of many crystallite orientations whose position simply depends on the orientation of the crystallite with respect to the magnetic field, then each crystallite is independent of its neighbor. Therefore, irradiation of a region of the lineshape does not alter the nonresonant crystallites. Sometimes mother nature can make the crystallites dependent on its neighbors, which in turn would render the lineshape as

homogeneous.[1] A simple example would be chemical exchange. We will come back to the point in a moment.

MAS techniques are highly effective in case of inhomogeneous line broadening due to chemical shift anisotropy in dilute spins or to an isolated heteronuclear spin system coupled by dipole-dipole interaction. A rule of thumb in MAS experiments is the lineshape should break into a pattern of spinning side bands as soon as spinning speed exceeds the line width of a given isochromate. In the case of an inhomogeneous lineshape for ^{13}C, that spinning speed is a few tens of Hz. In a uniformly enriched biological sample, the carbon spin has become more complicated, due to the presence of the homonuclear direct and indirect couplings. However, modest spinning speeds are sufficient to overcome the flip-flop terms due to the much smaller ^{13}C-^{13}C dipole couplings. It has been indicated in several recent publications that carbon transverse relaxation time has been improved by a factor of 3 at least for spinning speed above 40 kHz in uniformly isotope labeled proteins. In the case of ^{1}Hs the homogeneous lineshape makes it appear that the line width of a given isochromate is the width of the full powder pattern. The full width can be > 60 kHz. One can now appreciate why spinning at greater than 100 kHz is needed to begin to achieve a high resolution ^{1}H spectrum.[2]

Current state-of-the-art MAS probes can reach above 120 kHz MAS and it is still a point of argument how fast the sample should spin to completely break down the ^{1}H dipolar network. Before we develop a way of making the ^{1}H MAS of proteins more appealing, it is worthwhile describing some of the technical features needed to accomplish such high spinning speeds.

In recent publications[2], fully protonated proteins spun at 111 kHz MAS producing a single proton resonance linewidth at half maximum between 100-200 Hz for amide and aliphatic protons, though it is not fully clear how much of this arises from inhomogeneous broadening mechanisms that are proportional to B_0, some of which are related to materials used for susceptibility matching of the rf coil. One of the major drawbacks in applying fast MAS is that rotor size decreases as the spinning speed increases. Commercially available fast MAS probes with 1.3 mm (OD) and 0.7 mm (OD) can spin rotors up to a maximum of 67 kHz and 111 kHz, respectively (Bruker Biospin). However, as the size of the rotor decreases, the effective sample volume decreases as well, from 3 μL (~2-3 mg sample) to ~300 nL (~200 μg sample). Although fast MAS enables ^{1}H detection, sensitivity per unit time is still a concern. The positive advantages of going to very fast MAS are: (1) sensitive ^{1}H detection is potentially enabled with better resolution with sub-milligram samples; (2) fast MAS improves coherence life time (improved T_2) of low gamma nuclei including quadrupolar nuclei; (3) the micro coils used for RF irradiation can generate short pulses at low power, enabling rapid data collection for molecules with short longitudinal relaxation time; and (4) the fast spinning reduces decoupling requirements and thus reduces sample rf heating.

Irrespective of all advantages and sample amount limitations, ^{1}H's isotropic line shape analysis in fast MAS of protonated samples is still complicated. Some of the facts taken from earlier publications are summarized below.

The isolation of the spins exhibited by ^{13}C is in contrast to the behavior of the ^{1}H lineshape in the presence CW rf irradiation. The ^{1}H spin system is significantly more complicated. Like the ^{13}C

lineshape, it has an anisotropic shielding contribution. At higher magnetic field, chemical shift anisotropy and homo-nuclear dipolar coupling strengths can become comparable. Additionally, there exists indirect J-couplings although much smaller than the direct dipole-dipole interactions, they are isotropic in nature and hence are not removed under MAS. A closer look at the direct dipole-dipole interaction is worthwhile. The dipole-dipole Hamiltonian is given by

$$\mathcal{H}_{ij}^{DD} = \frac{\mu_0 \gamma_i \gamma_j \hbar}{4\pi} \left[(I_i \cdot I_j) r^{-3} - 3(\vec{I_i} \cdot \vec{r})(\vec{I_j} \cdot \vec{r}) r^{-5} \right]$$

In polar coordinates, the Hamiltonian is expressed as

$$\begin{aligned} \mathcal{H}_{ij}^{DD} = \frac{\mu_0 \gamma_i \gamma_j \hbar}{4\pi r^3} [& (1 - 3cos^2\theta) I_{iz} I_{jz} - \tfrac{1}{4}(1 - 3cos^2\theta)\{I_i^+ I_j^- - I_i^- I_j^+\} \\ & - \tfrac{3}{2}sin\theta\ cos\theta\ e^{-i\varphi}\{I_i^+ I_{jz} + I_j^+ I_{iz}\} - \tfrac{3}{2}sin\theta\ cos\theta\ e^{i\varphi}\{I_i^- I_{jz} + I_j^- I_{iz}\} \\ & - \tfrac{3}{4}sin^2\theta\ e^{-i2\varphi} I_i^+ I_j^+ - \tfrac{3}{4}sin^2\theta\ e^{i2\varphi} I_i^- I_j^-] \end{aligned}$$

Where, θ and ϕ are Euler angles describing the orientation of dipolar vector with respect to the external magnetic field; γ, the gyromagnetic ratio; r, the inter-nuclear distance; ℏ, Planck's constant divided by 2π; μ_0 permeability constant. In the secular approximation, if the difference between the Larmor frequency of spin i and j is greater than the constant factor in the dipolar Hamiltonian, i.e. $\omega_{0i} - \omega_{0j} \gg \frac{\mu_0 \gamma_i \gamma_j \hbar}{4\pi r^3}$, then we can neglect the last four terms in the Hamiltonian.

In the case of homonuclear coupling (like spins), the Hamiltonian can be rewritten as

$$\mathcal{H}_{ij}^{DD} = \frac{\mu_0 \gamma_i \gamma_j \hbar}{4\pi r^3} \tfrac{1}{2}(1 - 3cos^2\theta)[3\ I_{iz} I_{jz} - \vec{I_i} \cdot \vec{I_j}]$$

In the case of heteronuclei, the Hamiltonian is further reduced to

$$\mathcal{H}_{ij}^{DD} = \frac{\mu_0 \gamma_i \gamma_j \hbar}{4\pi r^3} (1 - 3cos^2\theta)\ I_{iz} I_{jz}$$

The first point to notice is that the first two terms in the dipole-dipole interactions depend upon the "$3cos^2\theta - 1$". If we can zero that term, the strong dipole-dipole coupling would disappear. This was the driving force for the initial magic angle spinning (MAS) experiments by Andrews[3] and Lowe.[4] It is Magic because the angle given by cos[-1][$\frac{1}{\sqrt{3}}$], causes the dipole-dipole term to disappear. However, the average Hamiltonian for an isolated homonuclear two spins with definite isotropic chemical shift difference, chemical shift anisotropy, and dipolar coupling can be rewritten as[5]

$$\mathcal{H}_{ij}^{avg} = -\omega_i\ I_{zi} - \omega_j\ I_{zj} + J\ I_{iz} I_{jz} + i\tfrac{k}{2}\{I_i^+ I_j^- - I_i^- I_j^+\}$$

Where, k is a constant that is directly proportional to the chemical shift anisotropy (σ) and dipolar interaction (D), and is inversely proportional to the MAS frequency (v_r). More importantly this constant factor k characterizes the lineshape.

If the isotropic chemical shift difference, $\Delta\delta_{iso} = \frac{1}{2\pi}(\omega_i - \omega_j)$, is small compared to k, the line shape and width varies proportionally with respect to (D·σ/v_r). On the other hand, if $\Delta\delta_{iso} >$ k, the line shape and width vary proportionally with respect to the square of k.

In a protonated molecule or a protein, [1]Hs are coupled to each other and form a dipolar network. It is not trivial to draw any conclusion on linewidths measured from numerous samples under very fast MAS. It has been shown recently[6] that the linewidth and lineshape of [1]Hs have a linear to quadratic dependency on the spinning speed. For inhomogeneous broadening, an increase in the spinning speed reduces anisotropic peak linewidth linearly, until the natural linewidth is obtained. However, for homogeneous broadening the reduction in linewidth is better described by a quadratic relation.

Hence a semi-empirical quadratic equation is derived to describe the linewidth of proton resonances as a function of isotropic chemical shift difference and constant factor k~ D·σ/v_r.

$$\Delta w \sim \frac{1}{\Delta\delta_{iso}}(k + k^2)$$

Why Deuterate your sample?

From the preceding discussion it is clear that if we can dilute the ^{1}H network by introducing low gamma nuclei such as ^{2}H, it is possible to mitigate much of the strong homonuclear dipolar interactions, thus affording higher resolution in the ^{1}H spectrum. Deuteration, effectively lowers the probability that two [1]Hs will be close to one another. However, there is drawback to deuteration which limits the resolution obtained in the ^{1}H spectrum. Namely, the introduction of indirect isotropic [1]H-[2]H J-coupling and isotope shifts. In such cases, moderate spinning will reduce the weaker dipolar interactions, but will not mitigate the J-coupling or the chemical shift dispersion due to secondary isotope effects which will appear as a line broadening process. With a need for only modest spinning rates, larger rotors can be employed. The [1]H-[2]H J-coupling can easily be removed, *via* [2]H-decoupling. However, the consequences of the secondary isotope effects will still be present. The obvious cost being larger rotors means more sample is needed. For example, a 3 mm rotor will use between 10 and 30 mg of protein.

If the end user cannot afford that much sample, then it is clear the utilization of small diameter rotors will enable the user's experiments. However, if the larger samples are possible, then as hinted above other opportunities come into play. To illustrate the different opportunities, we have performed a series of experiments utilizing the protein GB1.

The sample, 12-15 mg U-^{13}C, ^{15}N, ^{2}H labeled GB1, was packed into a 3mm silicon nitride rotor using spacers. The spacers were of a size to place the sample in the center of the coil. The rotor was spun at 25 kHz MAS while the sample temperature was maintained near 12±2 ˚C by passing nitrogen gas through an AirJet refrigerator system (SP Scientific). The 2D spectrum consists of nearly 58 distinguishable peaks. Each peak corresponds to single-bonded proton-nitrogen nuclei in back bone and side chains. However, 6 resonances arose from amino acid side chains (Lys, Trp, Asn, Gln), thus leaving 52 cross peaks from backbone residues. This demonstrates that the current spectrum has resolved nearly 94% of the amino acids in the protein sequence. The average line-width at half maximum for proton and nitrogen is 70±10 Hz and 40±5 Hz

respectively. For illustration purposes (see Figure 1), proton and nitrogen 1D slices are shown in magenta. The maximum SNR of a single cross-peak is ~70:1.
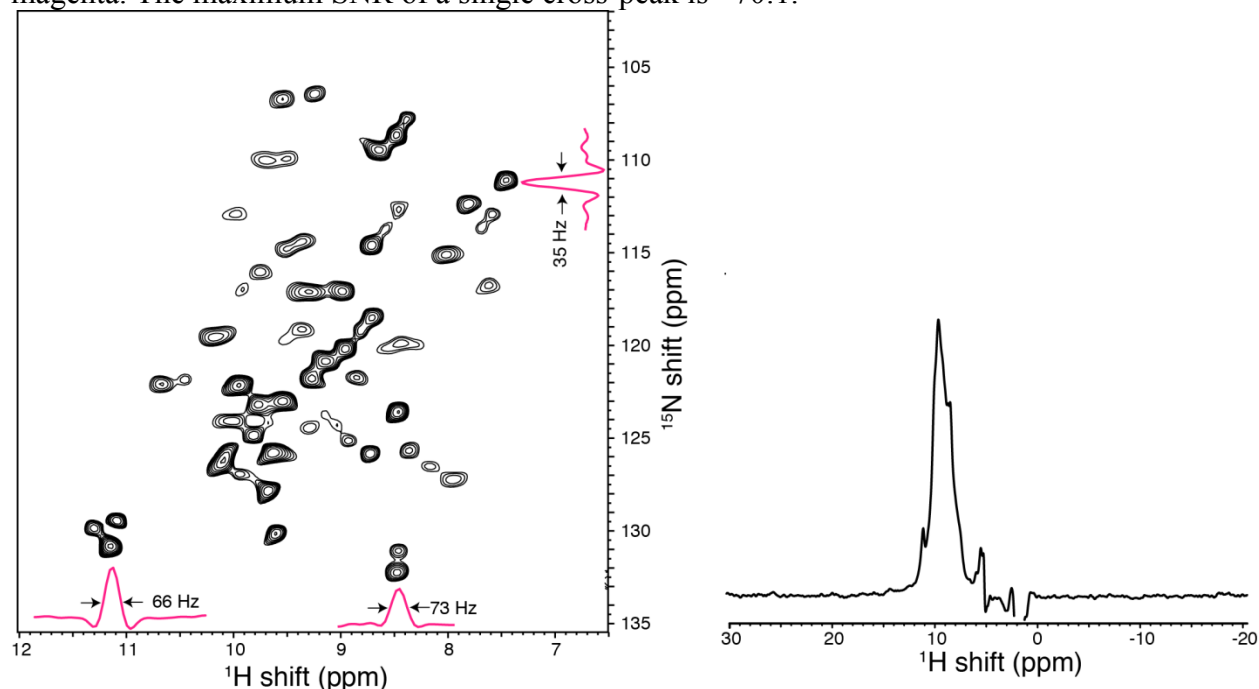
Figure 1: Inverse proton detected ^{1}H/^{15}N heteronuclear correlation 2D- spectrum of U-C, D, N labeled GB1 obtained with a Doty 3 mm HXYZ MAS probe operating in a 500 MHz JEOL spectrometer. 12-15mg of micro/nano-crystalline protein samples were center packed using spacers and spun at 25 kHz MAS. Two transients were co-added for each indirect increment (total 64), with a 2 second recycle delay. Total experiment time was <5 min. 2D data was zero filled to at least four times and sine apodization function was applied prior to Fourier transformation in both dimensions. A proton 1D-spectrum of the first FID from the 2D experiment is shown to the right. 1D data was processed with 100 Hz line broadening and measures SNR ~250:1 for two scans.

Discussion

The first FID of the 2D spectrum measures SNR ~250:1 for two scans for the current experimental conditions, as presented in Figure 1 above. This is in contrast to what has been reported in the literature.[7] In that case the 1.3 mm and 0.7 mm probes have similar sensitivity (SNR 46:1 for 4 scans) although the sample volume for 1.3 mm rotor is 4-5 times larger than that of the 0.7mm rotor as described in the article by Andreas[7]. The first FID of a proton detected 2D experiment on either deuterated GB1 (1.3mm probe and 60 kHz MAS) or protonated GB1 (0.7 mm probe and 111 kHz MAS) protein measures a SNR 46 :1 for four scans. Note that the fast MAS measurements are carried out on a 1 GHz spectrometer which typically has ~3 times the sensitivity per sample mass of a 500 MHz spectrometer for a constant linewidth, though this ratio depends strongly on details of the probe designs.

The best expression for predicting and comparing sensitivities for similar samples on different probes at different fields and temperatures is the following:

$$\text{S/N} \propto 1000 \left[\frac{\hbar^2}{48 K_B^{3/2}} \pi \sqrt{\mu_0} \right] I(I+1) \left[\frac{n_S \, V_S \omega^2 \sqrt{T_2^*}}{\tau_{90} T_S \sqrt{P(T_R + T_P)}} \right]$$

where n_s is the relative number of spins per site (or degree of protonation for a given site), V_S is the sample volume, P is the power required to achieve a $\pi/2$ pulse length of τ_{90}, T_S is the sample temperature, T_R is the probe noise temperature (in most probes close to RT even when the sample is cold), and T_P is the preamp noise temperature (usually ~100 K), K_B is the Boltzmann constant, $\hbar$ is Planck's constant divided by 2π, μ is the permeability in free space. The sample volumes of the three probes are approximately 35μL, 3μL, and 0.5μL for the Doty 3mm, Bruker 1.3 mm, and Bruker 0.7 mm, respectively. Not knowing the $B_1/P^{0.5}$ performance of the Bruker probes limits our ability to be very quantitative in comparing SNR of our probes to that of Bruker probes, but the following table shows relative SNR that can be expected from probes that we have built and tested, or carefully simulated in detail, for several different T2*s, sample temperatures, degrees of protonation, and probe noise temperatures, the last of which can be similar to the sample temperature in a new probe under development.

Probe description	1H	rotor	MAS	Vs	pw90	P	Ts	ns	T2*	Tr	1H	k
	MHz	mm	kHz	uL	us	W	K	%	ms	K	SNR	
Doty 3mm NB HXYZ	500	3	26	35	3.9	80	285	30	4.5	280	177	31.0
Doty 3mm NB HXYZ	500	3	26	35	2	145	285	30	4.5	280	257	31.0
Doty-JRI 1mm NB HXY	700	1	70	1	1.2	40	285	99	2.2	290	75	31.0
Doty 1.3mm NB HXYZ	800	1.3	70	3.5	2.5	45	285	30	3.8	280	55	31.0
Doty 3mm NB HXYZ	800	3	28	35	2.8	130	285	30	4.5	280	310	31.0
Doty 3mm NB HXYZ	800	3	28	35	2.8	130	285	99	1.9	280	670	31.0
Doty-JRI 0.75mm NB HXY	900	0.75	115	0.26	0.9	80	285	99	1.9	290	22	31.0
Doty 0.7mm NB HXYZ	1200	0.7	120	0.5	1.3	25	280	99	1.9	280	72	31.0

The right most column in Table 1 shows a range of a factor of 30 from lowest to highest calculated ^{1}H SNR for various probes and conditions. We note that we have seen significantly lower rf efficiencies in older probe circuit designs. The first two entries in the Table for a Doty 3mm NB HXYZ probe illustrate how widely differing efficiencies can be for the same probe, depending on circuit details and optimization strategies. The values at 500 MHz, 700 MHz, and 900 MHz are from detailed probe circuit simulations that were validated by experimental test data. The values at 800 MHz and 1200 MHz are from detailed probe circuit simulations only. All assume biological sample loads. The reported SNR on the Bruker 1.3-mm probe at 1 GHz suggests its rf circuit efficiency was much lower than what we have seen in our recent small-sample single-solenoid HXY probes at 700 and 900 MHz, though that is contrary to some other notes we've seen. The increased linewidth from the slower spinning of the 1.3-mm 1 GHz probe does not begin to account for its low reported SNR. We simply cannot explain its anomalously low reported SNR, but we note that the SNR reported for the 0.7-mm Bruker probe is consistent with our expectations.

The quad probe and multinuclear detection

A newly developed Doty 3 mm H-F/X/Y/Z quad tuned MAS probe enables state-of–the-art NMR technology. The MAS probe is designed with a single solenoid RF resonator that is capable of tuning to four different frequencies ranging from 10 MHz to 800 MHz (and eventually to 1.3 GHz with 1.3-mm rotors). The maximum spinning speed can reach up to 28 kHz while pulsing on four channels with duty cycle such that accommodates an average power up to 10 W. For the purposes of the present discussion, we demonstrate the performance of the four channel MAS probe, quad-MAS, on a variety of samples (liquids, viscous liquids, and solids) in Figure 2; also, a microcrystalline protein sample in Figure 1.

Resolution and sensitivity of the Quad-Fast-MAS probe are demonstrated by applying tailored experiments (single pulse to CPMAS) for multi-nuclear detection. Figure 2 represents one-dimensional spectra obtained from liquids like fluorinated polymers, viscous liquids, and polycrystalline solids. The probe was quad-tuned to ^{1}H-^{19}F/^{13}C/^{15}N/^{2}H.

For ^{19}F NMR in Figure 2A, the high frequency channel is tuned to 470 MHz and a single pulse (90 pulse width 3.5 us at 75 W) was applied to record ^{19}F spectrum of 10 μL perfluorocarbon polymer (5 crown ether). The peak width at half maximum is 10 Hz. With 4 scans data accumulation ^{19}F SNR measures >40,000. Sample was spun at 5 kHz MAS.

Figure 2: Multi-nuclear NMR spectra obtained from 500 MHz JEOL spectrometer equipped with DSI 3mm quad-MAS probe.

Figure 2B represents ^{1}H/^{15}N CPMAS, conducted at 22 kHz MAS with co-addition of 8 transients to reproduce the spectrum. A fully packed rotor with (~25 mg) ^{15}N labeled alanine polycrystals was used for the measurement of pulse widths and S/N. RF nutation data measures a 6 μs 90 pulse width at ~300 W. The ^{15}N SNR is ~203 without applying any line broadening function during data processing.

Figure 2C presents deuterium NMR spectrum of 99% deuterated Proline polycrystals recorded at 20 kHz MAS. A single respiration pulse (four pulses with 2μs each over four rotor periods, 8 μs for 90-degree flip) at 300 W was applied and 8 transients were coadded to measure the family of spinning sidebands originating from the deuterium powder pattern.

Figure 2D shows ^{1}H-^{13}C CPMAS spectrum of gycine at natural abundance. A 30 mg sample was center packed using spacers. CP/MAS conditions were, 1ms CP contact time and 30 ms acquisition under 80 kHz proton decoupling. 32 transients were co-added and no line broadening or apodization function was applied during processing.
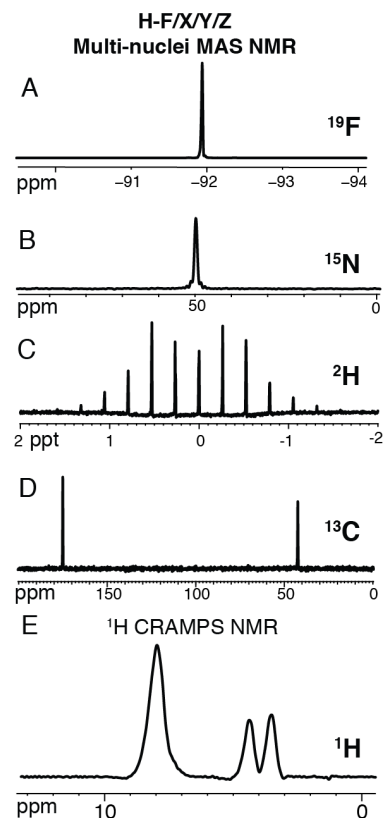
Figure 2E is a single scan ^{1}H CRAMPS spectrum of glycine (center packed) obtained under amplitude modulated PMLG-3 windowed acquisition.

An experiment carried out on a viscous liquid sample is shown in Figure 3. Here, 4-cyano-4' pentyl biphenyl (5cb) liquid crystal was used to record a proton detected 1H/13C HSQC-2D spectrum. The 30 µL fully packed rotor was spun at 5 kHz MAS to obtain a high-resolution proton spectrum from 5cb in nematic phase at room temperature (^{1}H linewidth is ~28 kHz for non-spinning rotors). Standard inverse detected 2D HSQC pulse sequence (similar to solution NMR) was applied to record the 2D spectrum with four scans per increment. Each cross-peak corresponds to chemical shift of singly bonded ^{1}H and ^{13}C nuclei.

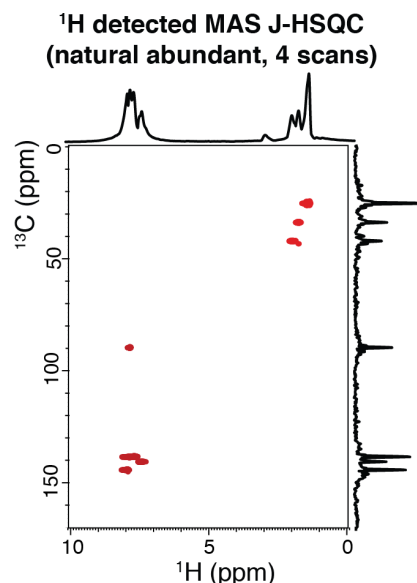## High-resolution ^{1}H detection with ^{2}H decoupling.

The sample coil is accurately compensated for zero susceptibility to permit high resolution ^{1}H MAS spectra. The B_0 homogeneity in the sample volume is illustrated in Figure 4, with the one-dimensional proton spectrum obtained from isopropanol and deuterated MPD used in GB1 protein sample.

^{1}H detected MAS J-HSQC (natural abundant, 4 scans)

Figure 3: Inverse proton detected 2D HSQC spectrum of 5cb in natural abundance obtained from a 500 MHz JEOL spectrometer.

Figure 4 summarizes single pulse ^{1}H spectra obtained with or without ^{2}H decoupling. One pulse ^{1}H spectrum is shown in Figure 4A without ^{2}H decoupling.
The H_2O peak is denoted at ~5ppm. Expanded region (1-2 ppm) from A is shown in C. Figure 4B represents ^{2}H decoupled one pulse ^{1}H spectrum. Water proton magnetization was saturated by applying a low power pre-saturation pulse of 0.5s length. Figure 4D is the expanded region of B. Proton linewidths are marked for visual guidance. Note that without ^{2}H decoupling the proton peaks are ~ 10 Hz broad due to two-bond

Figure 4: ^{1}H NMR spectra of GB1 sample obtained at 20 kHz MAS with or without ^{2}H decoupling.

[1]H/[2]H J-coupling in CHD2, CH2D moieties. Each attached ^{2}H splits the ^{1}H peak into three separated by ~2 Hz. A single peak will split into five when two deuterium nuclei are attached, resulting in a linewidth of ~10 Hz. However, the line can be narrowed to 3 Hz with ^{2}H decoupling.".
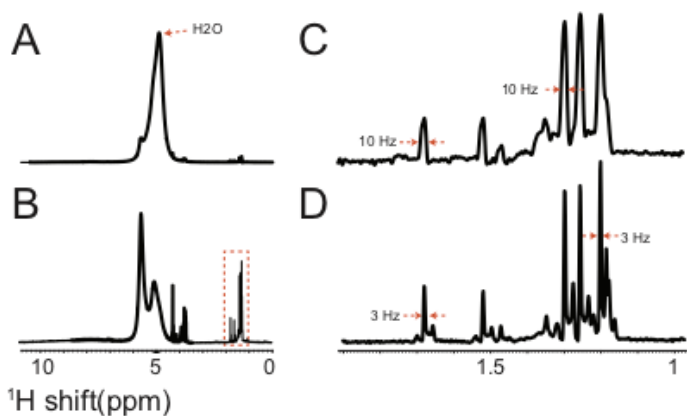
Summary

In this white paper, we have experimentally demonstrated high resolution proton-detection NMR experiments from deuterated proteins under moderate spinning. We have also discussed, line narrowing effect under MAS is dependent on various conditions including samples, probes, and experimental conditions. Experimental data indicates that very fast MAS (> 100 kHz) remarkably narrows proton line widths from fully protonated samples and increase transverse relaxation time for all nuclei, but absolute sensitivity of experiments is limited by the sample quantity. On the other hand, moderate spinning (~25 kHz) is sufficient to narrow proton lines from perdeuterated proteins, which is in good agreement with previous publications. It is also experimentally demonstrated sensitivity per scan per time is ~8 times higher for a 3mm probe compared to fast MAS experiments in 1.3mm and 0.7mm probes. We have also demonstrated the efficacy of the 3mm ^{1}H-^{19}F/^{13}C/^{15}N/^{2}H quad-MAS probe with detection of high-resolution spectra from solution, semi solids, and solids. Notably, examples are shown from ^{19}F detection from liquid like fluorinated polymers, ^{1}H under ^{2}H decoupling from a biological sample, inverse ^{1}H detected ^{1}H/^{13}C HSQC spectrum from 5cb liquid crystals in natural abundance, ^{13}C and ^{15}N CP-MAS, and ^{1}H CRAMPS from microcrystalline powder samples. We also expect to demonstrate the experimental capabilities of the probe with detection of other combinations of nuclei and resolution and sensitivity enhanced multi-dimensional experiments under ^{2}H decoupling.

Acknowledgement

References
1. Portis, A. M., Electronic Structure of F Centers: Saturation of the Electron Spin Resonance. Physical Review 1953, 91 (5), 1071 - 1078.
2. Andreas, L., Le Marchand, T., Jaudzems, K., Pintacuda, G, Higjh Resolution proton-detected NMR of proteins at very fast MAS. J > Magn Reson. 2015, 253, 36-49.
3. E.R. Andrew, A. B., R.G. Eades, Nuclear Magnetic Resonance Spectra from a crystal rotated at high speed. Nature 1958, 182 (4650), 1659.
4. Lowe, I. J., Free Induction Decays of Rotating Solids. Phys. Rev Lett 1959, 2 (7), 285 - 287.
5. Gan Z-H, G., D. M., et al, Mol. Phys. 1989, 67 (6), 1419.
6. U. Sternberg, R. W., I. Kuprov, J. M. Lamley, A. Oss, J. R. Lewandowski, A. Samoson, 1H line width dependence on MAS speed in solid state NMR - Comparison of experiment and simulation. J Magn Reson 2018, 291, 32 - 39.
7. Andreas, L. B., Jaudzems, K., Stanek, J., Lalli, D., Bertarello, A., Marchand, T.L., Paepe, D., C., Kotelovica, S., Akopjana, I., Knott, B., Wegner, S., Engelke, F., Lesage, A., Emsley, L., Tars, K., Herrmann, T., Pintacuda, G., Structure of fully protonated proteins by proton-detected magic angle spinning NMR. PNAS 2016, 113 (33), 9187 - 9192.